

increase the probability of noncentrosymmetric crystallization.

**Acknowledgment.** The research described in this paper was performed by the Jet Propulsion Laboratory, California Institute of Technology, as part of its Center for Space Microelectronics Technology, which is supported by the Strategic Defense Initiative Organization, Innovative Science and Technology Office, through an agreement with the National Aeronautics and Space Administration. S.R.M. thanks Professor Robert Grubbs for access to synthetic facilities at Caltech. The diffractometer used in this study was purchased with a grant from the National Science Foundation (CHE-8219039). We thank Paul Groves and Kelly Perry for technical assistance.

**Registry No.** 2, 129540-53-0; 4, 129540-63-2; 5, 129540-66-5; 6a, 129540-68-7; *m*-MeOC<sub>6</sub>H<sub>4</sub>CHO, 591-31-1; *p*-MeOC<sub>6</sub>H<sub>4</sub>CHO, 123-11-5; *p*-(CH<sub>2</sub>)<sub>4</sub>NC<sub>6</sub>H<sub>4</sub>CHO, 51980-54-2; *p*-Me<sub>2</sub>NC<sub>6</sub>H<sub>4</sub>CHO,

100-10-7; 2,4-(MeO)<sub>2</sub>C<sub>6</sub>H<sub>3</sub>CHO, 93-02-7; *o*-MeOC<sub>6</sub>H<sub>4</sub>CHO, 135-02-4; C<sub>6</sub>H<sub>5</sub>FeC<sub>5</sub>H<sub>4</sub>CHO, 12093-10-6; 2-CH<sub>3</sub>C<sub>5</sub>H<sub>4</sub>N<sup>+</sup>CH<sub>3</sub>·CF<sub>3</sub>SO<sub>3</sub><sup>-</sup>, 129540-51-8; 2-CH<sub>3</sub>C<sub>5</sub>H<sub>4</sub>N<sup>+</sup>CH<sub>3</sub>·Ts<sup>-</sup>, 2073-76-9; (*E*)-(CH<sub>3</sub>)<sup>+</sup>NC<sub>5</sub>H<sub>4</sub>CH=CHC<sub>6</sub>H<sub>4</sub>OMe-*p*-CF<sub>3</sub>SO<sub>3</sub><sup>-</sup>, 129540-55-2; (*E*)-(CH<sub>3</sub>)<sup>+</sup>NC<sub>5</sub>H<sub>4</sub>CH=CHC<sub>6</sub>H<sub>4</sub>N(CH<sub>2</sub>)<sub>4</sub>-*p*-CF<sub>3</sub>SO<sub>3</sub><sup>-</sup>, 129540-57-4; (*E*)-(CH<sub>3</sub>)<sup>+</sup>NC<sub>5</sub>H<sub>4</sub>CH=CHC<sub>6</sub>H<sub>4</sub>NMe<sub>2</sub>-*p*-CF<sub>3</sub>SO<sub>3</sub><sup>-</sup>, 129540-59-6; (*E*)-2,4-(MeO)<sub>2</sub>C<sub>6</sub>H<sub>3</sub>CH=CH<sup>+</sup>NC<sub>5</sub>H<sub>4</sub>(CH<sub>3</sub>)·CF<sub>3</sub>SO<sub>3</sub><sup>-</sup>, 129540-61-0; (*E*)-C<sub>6</sub>H<sub>5</sub>FeC<sub>5</sub>H<sub>4</sub>CH=CHN<sup>+</sup>C<sub>5</sub>H<sub>4</sub>(CH<sub>3</sub>)·CF<sub>3</sub>SO<sub>3</sub><sup>-</sup>, 129540-70-1; (*E*)-C<sub>6</sub>H<sub>5</sub>FeC<sub>5</sub>H<sub>4</sub>CH=CHN<sup>+</sup>C<sub>5</sub>H<sub>4</sub>(CH<sub>3</sub>)·Ts<sup>-</sup>, 129570-18-9; (*E*)-C<sub>6</sub>H<sub>5</sub>NC<sub>5</sub>H<sub>4</sub>CH=CHN<sup>+</sup>C<sub>5</sub>H<sub>4</sub>(CH<sub>3</sub>)·I<sup>-</sup>, 129540-71-2; (*E*)-C<sub>6</sub>H<sub>5</sub>NC<sub>5</sub>H<sub>4</sub>CH=CHN<sup>+</sup>C<sub>5</sub>H<sub>4</sub>(CH<sub>3</sub>)·Br<sup>-</sup>, 129540-72-3; (*E*)-*p*-Me<sub>2</sub>NC<sub>6</sub>H<sub>4</sub>CH=CHN<sup>+</sup>C<sub>5</sub>H<sub>4</sub>(CH<sub>3</sub>)·BF<sub>4</sub><sup>-</sup>, 129540-64-3.

**Supplementary Material Available:** Details of data collection, treatment, structure solution, refinement, an ORTEP drawing of the cations of 2 and 4 with atom numbering, tables of crystal data, final parameters of all the atoms, and complete distances and angles (16 pages); observed and calculated structure factors (12 pages). Ordering information is given on any current masthead page.

## Molecular and Macroscopic Second-Order Optical Nonlinearities of Substituted Dinitrostilbenes and Related Compounds

Bruce G. Tiemann, Seth R. Marder,\* and Joseph W. Perry

Jet Propulsion Laboratory, California Institute of Technology, Pasadena, California 91109

Lap-Tak Cheng\*

Central Research and Development Department, E. I. du Pont de Nemours and Company Inc., Experimental Station, Wilmington, Delaware 19880-0356

Received April 17, 1990

A series of compounds of the form (*E*)-1-(2,4-dinitrophenyl)-2-R-ethylene, where R is a donor group, was prepared, and their molecular hyperpolarizabilities were examined by the dc electric-field-induced second-harmonic generation (EFISH) method. Although the compounds studied had charge-transfer bands at lower energy than their 4-nitrostilbene analogues, the EFISH-determined values of  $\beta_u$ , the vectorial projection of the hyperpolarizability tensor along the dipole moment direction, were reduced. The powder second harmonic generation efficiencies of these compounds were determined by the Kurtz powder technique.

### Introduction

The desire to exploit the second-order optical nonlinearities of conjugated organic materials<sup>1</sup> has led researchers to develop structure-properties relationships for hyperpolarizabilities.<sup>2</sup> Insights from these studies may provide guidelines for the synthesis of new highly nonlinear materials. To develop these relationships, it is important to experimentally determine the molecular hyperpolarizability tensor,  $\beta$ . The vectorial projection of  $\beta$  along the molecular dipole direction, denoted  $\beta_u$ , can be obtained by electric-field-induced second-harmonic generation (EFISH) experiments with relatively good accuracy.<sup>2,3</sup> Since  $\beta_u$  is

a frequency-dependent property, comparison of values measured for different molecules must account for dispersion, typically by using a model. An alternative approach, used in this study, is to perform measurements with sufficiently low frequency radiation so as to obtain an estimate of the limiting nonresonant value.

Second-order optical nonlinearities, such as second harmonic generation (SHG), can be observed only in materials lacking a center of symmetry.<sup>1a</sup> This usually precludes their observation in solutions since they are isotropic in the absence of some external perturbation. If the nonlinear chromophore (solute) is dipolar, application of an electric field causes each dipole to partially align with the field. This alignment removes the center of symmetry, allowing for the observation of second harmonics. If the ground-state dipole is oriented in a direction along which the projection of  $\beta$  contains the dominating components, then analysis of data from the EFISH experiment will provide a meaningful measure of the quadratic optical nonlinearity of the molecule. These measurements, coupled with theoretical models, facilitate a better understanding of the factors that lead to large hyperpolarizability.

(1) See, for example: (a) Williams, D. J. *Angew. Chem., Int. Ed. Engl.* 1984, 23, 690. (b) *Nonlinear Optical Properties of Organic and Polymeric Materials*; Williams, D. J., Ed.; ACS Symposium Series, 233; American Chemical Society: Washington, DC, 1983. (c) *Nonlinear Optical Properties of Organic Molecules and Crystals*; Chemla, D. S., Zyss, J., Eds.; Academic Press: Orlando, 1987; Vols. 1 and 2.

(2) (a) Oudar, J. L.; Chemla, D. S. *J. Chem. Phys.* 1977, 66, 2664. (b) Levine, B. F.; Bethea, C. G. *J. Chem. Phys.* 1977, 66, 2664. (c) Lalama, S. J.; Garito, A. F. *Phys. Rev. A* 1979, 20, 1179.

(3) (a) Oudar, J. L.; Le Person, H. *Opt. Commun.* 1975, 15, 268. (b) Levine, B. F.; Bethea, C. G. *Appl. Phys. Lett.* 24, 445. (c) Singer, K. D.; Garito, A. F. *J. Chem. Phys.* 1981, 75, 3572.

Theoretical models for individual tensorial components of  $\beta$  can be derived from perturbation theory, which leads to a sum over states formulation where

$$\beta_{ijk} \propto \sum_n \sum_{n'} \frac{\mu_{gn}^i \mu_{nn'}^j \mu_{n'g}^k}{E_{ng} E_{n'g}}$$

where  $i$ ,  $j$ , and  $k$  are coordinates,  $\mu_{gn}$  and  $\mu_{n'g}$  are the transition dipole moments between the ground state ( $g$ ) and excited states ( $n$  or  $n'$ ),  $\mu_{nn'}$  is the transition dipole moment between two excited states, and  $E_{ng}$  and  $E_{n'g}$  are energy denominators determined by the energy gaps between electronic states and the perturbation frequency.<sup>2,4</sup> For donor-acceptor-substituted benzenes such as 4-nitroaniline, it was found that a two-state model, in which a single charge-transfer excited state dominated the above expression, reasonably accounted for the observed  $\beta_\mu$  values.<sup>2a,5</sup> In this two-state approximation, the expression for the dominating components of  $\beta_\mu$  reduces to

$$\beta_{xxx} \propto (\mu_{nn} - \mu_{gg})(\mu_{gn}^x)^2 / E_{ng}^2$$

For donor-acceptor molecules, measurements of solvatochromic behavior of low-energy charge-transfer bands, which give an estimate of  $\mu_{nn} - \mu_{gg}$ , and their extinction coefficients, which relate to  $\mu_{ng}^2$ , serve as simple means for the evaluation of  $\beta_{xxx}$ , where  $x$  is essentially the charge-transfer direction.<sup>6</sup>

Theoretical<sup>2</sup> and experimental<sup>3</sup> studies have demonstrated significant enhancement of hyperpolarizability with extended conjugation. More recent studies have therefore focused on systems such as polyenes,<sup>7</sup> tolans,<sup>8</sup> and stilbenes<sup>8a,9</sup> in which the donor and the acceptor are separated by a longer conjugated linker than in the previously studied disubstituted benzenes. Recent EFISH studies on various donor-acceptor stilbenes indicated that the two-state model may be an oversimplification for these systems,<sup>10</sup> and therefore evaluation of  $\beta_\mu$  from solvatochromic effects may be misleading.

Qualitative structural modifications have been proposed as a means to manipulate  $\beta_\mu$ , including (a) variation of the strength of the donors and acceptors, (b) their relative positions, (c) the length of the conjugated bridge (d) its structure, and finally, (e) the number of donors and acceptors. In this paper we report the effect of multiple donors or acceptors on the molecular hyperpolarizabilities of a series of dinitrostilbenes and related compounds. We also report their macroscopic powder SHG efficiencies.

## Experimental Section

**Materials:** reagent grade methanol, acetone, diethyl ether, hexanes, and dichloromethane were purchased from Fisher Scientific and were used without purification. 2,4-Dinitrotoluene (97%), ferrocenecarboxaldehyde (98%), 1-pyrenecarboxaldehyde

**Table I. Summary of Reagents and Yields for 2,4-(O<sub>2</sub>N)<sub>2</sub>C<sub>6</sub>H<sub>3</sub>CH=CHX Compounds Starting with 1 g (5.5 mmol) of 2,4-Dinitrotoluene**

X	aldehyde		product	
	g	mmol	g	% yield
2-CH <sub>3</sub> OC <sub>6</sub> H <sub>4</sub>	1.5	11	0.55	33
4-CH <sub>3</sub> OC <sub>6</sub> H <sub>4</sub>	1.5	11	0.53	32
2,4-(CH <sub>3</sub> O) <sub>2</sub> C <sub>6</sub> H <sub>3</sub>	1.9	11	1.1	61
C <sub>18</sub> H <sub>9</sub> (1-pyrenyl)	1.67	7.3	0.17	8
4-(CH <sub>3</sub> ) <sub>2</sub> NC <sub>6</sub> H <sub>4</sub>	1.64	11	1.0	58
4-(CH <sub>3</sub> ) <sub>2</sub> NC <sub>6</sub> H <sub>4</sub> CH=CH	1.78	10	0.75	40
C <sub>5</sub> H <sub>5</sub> FeC <sub>5</sub> H <sub>4</sub> <sup>a,b</sup>	2.4	11	1.0	48

<sup>a</sup> Reaction performed under argon. <sup>b</sup> It was necessary to chromatograph the crude product on alumina with CH<sub>2</sub>Cl<sub>2</sub>/hexane. The product appeared as a greenish band on the column.

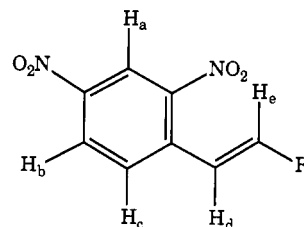


**Figure 1.** Labeling scheme for compounds in Table II.

(99%), 4-(dimethylamino)benzaldehyde (98%), 4-(dimethylamino)cinnamaldehyde (98%), and piperidine (99%) were obtained from Aldrich Chemical Co. and were used without purification. 2,4-Dimethoxybenzaldehyde was obtained from Lancaster Chemical Co. and was used without purification. Anisaldehyde was obtained from Eastman Chemical Co. and was used without purification. [<sup>2</sup>H<sub>6</sub>]Acetone (99.9% <sup>2</sup>H) was obtained from Cambridge Isotope Laboratories, and [<sup>2</sup>H]chloroform (99.9% <sup>2</sup>H) was obtained from Aldrich Chemical Co.; both were used without purification.

<sup>1</sup>H spectra were recorded on a Bruker AM-500 spectrometer. Chemical shifts were referenced to the chemical shift of the residual protons of the solvent with respect to tetramethylsilane. UV-visible spectra were recorded on a Hewlett-Packard 8154A diode array spectrophotometer. Elemental analyses were performed by the California Institute of Technology Analytical Facility.

**Synthesis. Sample procedure for the synthesis of 2,4-(O<sub>2</sub>N)<sub>2</sub>C<sub>6</sub>H<sub>3</sub>CH=CHX compounds:** 2,4-Dinitrotoluene (1 g, 5.5 mmol) and (dimethylamino)benzaldehyde (1.64 g, 11 mmol) were heated (80 °C) and stirred in a mixture of piperidine (3 mL) and toluene (10 mL) for 6 h. The precipitate was isolated by filtration, washed with hexanes, and air dried; yield 1.0 g, 58%, as dark, glistening blades.

Table I contains a summary of reagents and yields for 2,4-(O<sub>2</sub>N)<sub>2</sub>C<sub>6</sub>H<sub>3</sub>CH=CHX compounds, and Table II contains their NMR characterizations. Figure 1 shows the hydrogen labeling scheme for the compounds in Table II. Table III contains the elemental analyses of these compounds.

**Synthesis of 4'-[2-(hydroxymethyl)pyrrolidinyl]-2,4-dinitrostilbene:** 2,4-Dinitrotoluene (2.2 g, 12 mmol) and 4-[2-(hydroxymethyl)pyrrolidinyl]benzaldehyde<sup>11</sup> (5.0 g, 24.4 mmol), in toluene (30 mL), with piperidine (6 mL) were heated at 90 °C for 6 h. Maroon crystals were isolated in three crops totaling 3.87 g, 87% of which was pure by TLC. Recrystallization from CH<sub>2</sub>Cl<sub>2</sub>/pentane afforded analytically pure material. <sup>1</sup>H NMR (CD<sub>3</sub>COCD<sub>3</sub>)  $\delta$  8.70 (d,  $J$  = 2.2 Hz, 1 H, H<sub>a</sub>), 8.40 (dd,  $J$  = 9.0, 2.3 Hz, 1 H, H<sub>b</sub>), 8.24 (d,  $J$  = 8.9 Hz, 1 H, H<sub>c</sub>), 7.56 (d,  $J$  = 16.0 Hz, 1 H, H<sub>e</sub>), 7.51 (d,  $J$  = 8.8 Hz, 2 H, CHCHCN), 7.34 (d,  $J$  = 16.0 Hz, 1 H, H<sub>d</sub>), 6.71 (d,  $J$  = 8.3 Hz, 2 H, CHCN), 3.85 (dd,  $J$  = 8.0, 3.3 Hz, 1 H, CHCH<sub>2</sub>OH), 3.65 (dd,  $J$  = 11.0, 3.3 Hz, 1 H, CHHOH), 3.47 (dd,  $J$  = 9.7, 8.0 Hz, 1 H, CHHN), 3.40 (dd,  $J$  =

(4) (a) Ward, J. *Rev. Mod. Phys.* **1965**, *37*, 1. (b) Orr, B. J.; Ward, J. *F. Mol. Phys.* **1971**, *20*, 513.

(5) Oudar, J. L. *J. Chem. Phys.* **1977**, *67*, 446.

(6) (a) Levine, B. F.; Betheda, C. G.; Wasserman, E.; Leenders, L. J. *Chem. Phys.* **1978**, *68*, 5042. (b) Teng, C. C.; Garito, A. F. *Phys. Rev. B* **1983**, *28*, 6766.

(7) (a) Barzoukas, M.; Blanchard-Desce, M.; Josse, D.; Lehn, J. M.; Zyss, J. *Chem. Phys.* **1989**, *23*, 323. (b) Huijts, R. A.; Hesselink, G. L. *J. Chem. Phys. Lett.* **1989**, *156*, 209.

(8) (a) Tam, W.; Wang, Y.; Calabrese, J. C.; Clement, R. A. *Proc. SPIE* **1988**, *971*, 107. (b) Perry, J. W.; Stiegman, A. E.; Marder, S. R.; Coulter, D. R.; Beratan, D. N.; Brinza, D. E.; Klavetter, F. L.; Grubbs, R. H. *Proc. SPIE* **1988**, *971*, 17.

(9) Cheng, L. T.; Tam, W.; Stevenson, S. H.; Meredith, G. R.; Rikken, G.; Marder, S. R. *J. Am. Chem. Soc.*, submitted.

(10) Cheng, L. T.; Tam, W.; Meredith, G. R.; Rikken, G. L. J. A.; Meijer, E. W. *Proc. SPIE* **1989**, *1147*, 61.

(11) 4-[2-(Hydroxymethyl)pyrrolidinyl]benzaldehyde was prepared by heating prolinol with 4-fluorobenzaldehyde in DMF at 115 °C for 12 h, in the presence of K<sub>2</sub>CO<sub>3</sub>. The crude orange oil obtained after workup (~90% pure by <sup>1</sup>H NMR) was used without further purification.

**Table II. NMR Characterization of 2,4-(O<sub>2</sub>N)<sub>2</sub>C<sub>6</sub>H<sub>3</sub>CH=CHX Compounds**

for X = 2-C <sub>6</sub> H <sub>4</sub> OCH <sub>3</sub> : <sup>1</sup> H NMR (CD <sub>3</sub> COCD <sub>3</sub> ) δ 8.77 (d, <i>J</i> = 2.5 Hz, 1 H, H <sub>a</sub> ), 8.52 (dd, <i>J</i> = 8.8, 2.3 Hz, 1 H, H <sub>b</sub> ), 8.26 (d, <i>J</i> = 8.8 Hz, 1 H, H <sub>c</sub> ), 7.77 (d, <i>J</i> = 16.1 Hz, 1 H, H <sub>d</sub> ), 7.69 (dd, <i>J</i> = 6.2, 1.6 Hz, 1 H, =CHCCH), 7.69 (d, <i>J</i> = 16.2 Hz, 1 H, H <sub>d</sub> ), 7.38 (td, <i>J</i> = 7.8, 1.5 Hz, 1 H, CHCHCO), 7.09 (d, <i>J</i> = 8.1 Hz, 1 H, CHCO), 7.02 (t, <i>J</i> = 7.3 Hz, 1 H, CHCHCHCO), 3.93 (s, 3 H, OCH <sub>3</sub> )
for X = 4-C <sub>6</sub> H <sub>4</sub> OCH <sub>3</sub> : <sup>1</sup> H NMR (CD <sub>3</sub> COCD <sub>3</sub> ) δ 8.73 (d, <i>J</i> = 2.3 Hz, 1 H, H <sub>a</sub> ), 8.46 (dd, <i>J</i> = 8.8, 2.3 Hz, 1 H, H <sub>b</sub> ), 8.25 (d, <i>J</i> = 8.8 Hz, 1 H, H <sub>c</sub> ), 7.63 (d, <i>J</i> = 8.7 Hz, 2 H, CHCHCO), 7.56 (d, <i>J</i> = 16.2 Hz, 1 H, H <sub>d</sub> ), 7.47 (d, <i>J</i> = 16.1 Hz, 1 H, H <sub>d</sub> ), 6.99 (d, <i>J</i> = 8.7 Hz, 2 H, CHCO), 3.84 (s, 3 H, OCH <sub>3</sub> )
for X = 4-C <sub>6</sub> H <sub>4</sub> N(CH <sub>3</sub> ) <sub>2</sub> : <sup>1</sup> H NMR (CD <sub>3</sub> COCD <sub>3</sub> ) δ 8.70 (d, <i>J</i> = 2.4 Hz, 1 H, H <sub>a</sub> ), 8.41 (dd, <i>J</i> = 8.9, 2.4 Hz, 1 H, H <sub>b</sub> ), 8.24 (d, <i>J</i> = 8.9 Hz, 1 H, H <sub>c</sub> ), 7.56 (d, <i>J</i> = 16.2 Hz, 1 H, H <sub>d</sub> ), 7.53 (d, <i>J</i> = 8.7 Hz, 2 H, CHCHCN), 7.36 (d, <i>J</i> = 16.0 Hz, 1 H, H <sub>d</sub> ), 6.77 (d, <i>J</i> = 9.0 Hz, 2 H, CHCN), 3.03 (s, 6 H, NCH <sub>3</sub> )
for X = 2,4-C <sub>6</sub> H <sub>3</sub> (OCH <sub>3</sub> ) <sub>2</sub> : <sup>1</sup> H NMR (CD <sub>3</sub> COCD <sub>3</sub> ) δ 8.73 (d, <i>J</i> = 2.2 Hz, 1 H, H <sub>a</sub> ), 8.47 (dd, <i>J</i> = 8.8, 2.2 Hz, 1 H, H <sub>b</sub> ), 8.22 (d, <i>J</i> = 8.9 Hz, 1 H, H <sub>c</sub> ), 7.71 (d, <i>J</i> = 16.3 Hz, 1 H, H <sub>d</sub> ), 7.62 (d, <i>J</i> = 8.4 Hz, 1 H, =CHCHCO), 7.57 (d, <i>J</i> = 16.2 Hz, 1 H, H <sub>d</sub> ), 6.64 (d, <i>J</i> = 2.1 Hz, 1 H, OCCHCO), 6.62 (dd, <i>J</i> = 8.5, 2.2 Hz, 1 H, CHCHCO), 3.93 and 3.84 (both s, 3 H, OCH <sub>3</sub> 's)
for X = CH=CH-4-C <sub>6</sub> H <sub>4</sub> N(CH <sub>3</sub> ) <sub>2</sub> : <sup>1</sup> H NMR (CD <sub>3</sub> COCD <sub>3</sub> ) δ 8.70 (d, <i>J</i> = 2.3 Hz, 1 H, H <sub>a</sub> ), 8.41 (dd, <i>J</i> = 8.7, 2.5 Hz, 1 H, H <sub>b</sub> ), 8.22 (d, <i>J</i> = 8.8 Hz, 1 H, H <sub>c</sub> ), 7.50 (dd, <i>J</i> = 15.2, 10.5 Hz, 1 H, H <sub>d</sub> ), 7.45 (d, <i>J</i> = 8.8 Hz, 2 H, CHCHN), 7.04 (dd, <i>J</i> = 15.4, 10.7 Hz, 1 H, CH <sub>2</sub> CH), 7.00 (d, <i>J</i> = 15.1 Hz, 1 H, H <sub>d</sub> ), 6.92 (d, <i>J</i> = 15.5 Hz, 1 H, CH <sub>2</sub> CH=CH), 6.73 (d, <i>J</i> = 8.9 Hz, 2 H, CHCN), 3.00 (s, 6 H, NCH <sub>3</sub> )
for X = C <sub>6</sub> H <sub>4</sub> FeC <sub>5</sub> H <sub>5</sub> : <sup>1</sup> H NMR (CD <sub>3</sub> COCD <sub>3</sub> ) δ 8.71 (d, <i>J</i> = 2.4 Hz, 1 H, H <sub>a</sub> ), 8.44 (dd, <i>J</i> = 8.8, 2.4 Hz, 1 H, H <sub>b</sub> ), 8.23 (d, <i>J</i> = 8.8 Hz, 1 H, H <sub>c</sub> ), 7.49 (d, <i>J</i> = 15.9 Hz, 1 H, H <sub>d</sub> ), 7.17 (d, <i>J</i> = 15.9 Hz, 1 H, H <sub>d</sub> ), 4.68 and 4.47 (both t, <i>J</i> = 1.9 Hz, 2 H, CH of η-C <sub>5</sub> H <sub>4</sub> ring), 4.21 (s, 5 H, η-C <sub>5</sub> H <sub>5</sub> )
for X = pyrenyl: <sup>1</sup> H NMR (CD <sub>3</sub> COCD <sub>3</sub> ) δ 8.85 (d, <i>J</i> = 2.3 Hz, 1 H, H <sub>a</sub> ), 8.78 (d, <i>J</i> = 9.2 Hz, 1 H), 8.77 (d, <i>J</i> = 15.9 Hz, 1 H, H <sub>a</sub> ), 8.66 (d, <i>J</i> = 8.8 Hz, 1 H, H <sub>c</sub> ), 8.60 (ddd, <i>J</i> = 9.1, 2.3, 0.5 Hz, 1 H, H <sub>b</sub> ), 8.54 (d, <i>J</i> = 8.1 Hz, 1 H), 8.36 (d, <i>J</i> = 8.1 Hz, 1 H), 8.34 (d, <i>J</i> = 7.7 Hz, 2 H), 8.31 (d, <i>J</i> = 9.3 Hz, 1 H), 8.24 (d, <i>J</i> = 8.9 Hz, 1 H), 8.21 (d, <i>J</i> = 8.9 Hz, 1 H), 8.10 (d, <i>J</i> = 7.6 Hz, 1 H), 7.95 (d, <i>J</i> = 15.9 Hz, 1 H, H <sub>d</sub> )

**Table III. Elemental Analyses of 2,4-(O<sub>2</sub>N)<sub>2</sub>C<sub>6</sub>H<sub>3</sub>CH=CHX Compounds**

compd and formula	% C	% H	% N
for X = 2-C <sub>6</sub> H <sub>4</sub> OCH <sub>3</sub>			
calcd for C <sub>15</sub> H <sub>12</sub> N <sub>2</sub> O <sub>6</sub>	60.00	4.03	9.33
found	59.82	4.11	9.29
for X = 4-C <sub>6</sub> H <sub>4</sub> OCH <sub>3</sub>			
calcd for C <sub>15</sub> H <sub>12</sub> N <sub>2</sub> O <sub>6</sub>	60.00	4.03	9.33
found	60.17	4.19	9.23
for X = 2,4-C <sub>6</sub> H <sub>3</sub> (OCH <sub>3</sub> ) <sub>2</sub>			
calcd for C <sub>16</sub> H <sub>14</sub> N <sub>2</sub> O <sub>6</sub>	58.18	4.27	8.48
found	58.10	4.35	8.45
for X = <i>p</i> -C <sub>6</sub> H <sub>4</sub> N(CH <sub>3</sub> ) <sub>2</sub>			
calcd for C <sub>18</sub> H <sub>15</sub> N <sub>3</sub> O <sub>4</sub>	61.34	4.83	13.41
found	61.45	4.89	13.37
for X = CH=CH- <i>p</i> -C <sub>6</sub> H <sub>4</sub> N(CH <sub>3</sub> ) <sub>2</sub>			
calcd for C <sub>18</sub> H <sub>17</sub> N <sub>3</sub> O <sub>4</sub>	63.71	5.05	12.38
found	63.94	5.13	12.08
for X = 1-pyrenyl			
calcd for C <sub>24</sub> H <sub>14</sub> N <sub>2</sub> O <sub>4</sub>	73.09	3.58	7.10
found	73.36	3.92	6.98
for X = C <sub>6</sub> H <sub>5</sub> FeC <sub>5</sub> H <sub>4</sub>			
calcd for C <sub>18</sub> H <sub>14</sub> FeN <sub>2</sub> O <sub>4</sub>	57.17	3.73	7.41
found	57.16	3.81	7.41

11.0, 8.0, Hz, 1 H, CHHOH), 3.20 (dd, *J* = 9.3, 6.6 Hz, 1 H, CHHN), 2.15 and 2.00 (each m, 2 H, remaining CH<sub>2</sub>'s). Anal. Calcd. for C<sub>19</sub>H<sub>19</sub>N<sub>3</sub>O<sub>5</sub>: C, 61.78, H, 5.18, N, 11.38. Found: C, 61.67, H, 5.24, N, 11.41.

**Powder Second Harmonic Generation Measurements.** Measurements of the powder SHG efficiencies were performed by using the fundamental (1064 nm) of a Q-switched Nd:YAG laser (Quanta-Ray Model DCR-2A) or the first Stokes line (1907 nm) obtained by Raman shifting the Nd:YAG fundamental in H<sub>2</sub> gas. The appropriate excitation beam was selected and split into two beams, and each beam was long-pass filtered (using Schott RG-850 or RG-1000 filters) to remove stray radiation at the second-harmonic frequency. The beams were attenuated and weakly focused so as to deliver 100–500 μJ in a spot size of 2–3-mm diameter to the specimen under study. The two beams were used to excite a sample of the material to be measured and a powdered urea sample, the signal from which was used to provide a reference signal for normalization of shot-to-shot laser pulse amplitude fluctuations. The SH signals from the sample and the urea reference were analyzed by separate optical and electronic systems.

The excitation beams were incident on the samples at an angle of about 65°. The diffusely backscattered SH radiation was collected by using a 2-in. *f*/1.5 lens situated between the normal to the sample and the specularly reflected exciting beam. *f*/ $\pi$  matched lenses (*f*/3.5 or *f*/4) focused the collected light onto the

slits of monochromators (0.25 or 0.2 m with 6- or 10-nm bandpass). Schott KG-3 filters (for 1064-nm excitation) or water filters (for 1907-nm excitation) were used before the monochromators to eliminate collected excitation radiation.

The SH signals were detected by using photomultiplier tubes (Hamamatsu Models R928 or R406) whose outputs were amplified ( $\times 100$ , using two Comlinear CLC-100 amplifiers, dc 500-MHz bandwidth) and fed into boxcar integrators (Stanford Research Inc., Model SR-250). Typically, integrator gate widths of 10 ns were used. The outputs of the integrators were digitized by using an analog to digital converter (Analog Devices RTI 802) interfaced to a microcomputer (IBM PC-AT) which computed the normalized SH signal. True SH signals were distinguished from possible artifacts (fluorescence, inelastically scattered light, etc.) by tuning the monochromator to verify that the signal was narrowband around the SH frequency and by observing the signal in real time on a wide-bandwidth oscilloscope to ensure that only a prompt signal that essentially followed the laser pulse profile was observed.

Samples were unsized microcrystalline powders obtained by gently grinding materials with a mortar and pestle. The broad distribution of particle sizes was estimated to span from about 40 to 150 μm. Roughly 20 mg of powder was placed between glass microscope slide cover slips, the material was spread out to about 0.5 mm powder layer thickness, and the edges were sealed. Given the uncharacterized particle sizes and the possibility of preferential orientation of particles in assembling the samples, the uncertainties in the measured efficiencies can be quite large, perhaps factors of 2 or more, and therefore should be taken as a qualitative measurement.

**Dc Electric-Field-Induced Second Harmonic Generation Measurements.** The molecular hyperpolarizability,  $\beta$ , can be determined by using a methodology developed by Singer and Garito that involves a lengthy set of physical and optical measurements.<sup>3c</sup> These include, on a series of solutions with graded concentrations, measurements of density, refractive index at several wavelengths, solution capacitance, and also third harmonic generation (THG) and EFISH amplitudes and their coherence lengths. These measurements respectively determine the specific volume of a solute molecule in solution, solution dispersion, solution dielectric properties, and the THG and EFISH nonlinear susceptibilities for each solution. From these data  $\beta_{\mu}$  can be calculated.

The experimental setup for EFISH and THG consists of a 20-Hz Nd:YAG laser with 10-ns pulses of 0.4 J in energy. The 1064-nm output pumps a hydrogen Raman shifter, providing up to 120 mW of Stokes-shifted radiation at 1907 nm. This radiation serves as the fundamental frequency for both the EFISH and the THG experiments, with the harmonics at 954 and 636 nm, respectively. For most compounds with absorption edges at

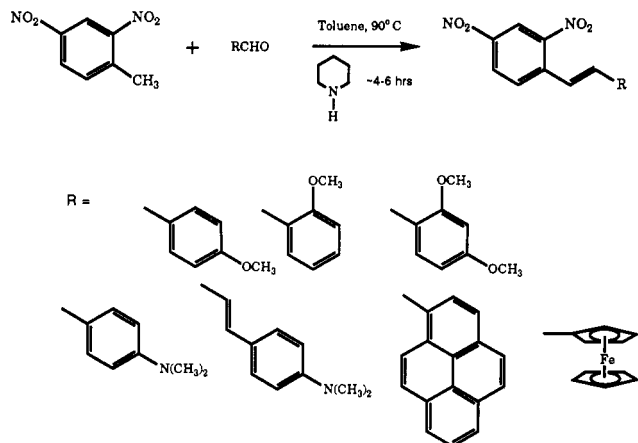


**Figure 2.** Synthesis of substituted dinitrostilbenes and related compounds.

wavelengths below 500 nm, the measurement can be considered not dispersively enhanced. THG and EFISH experiments are carried out with an unconventional technique in which the harmonic amplitudes and coherence lengths are measured separately. For the determination of harmonic amplitudes, we adopted a tight-focusing geometry in which the focal region of the laser beam is placed at the window-liquid interface of a "single interface" sample cell. The sample cell is equipped with a thick (2 cm) front optical window (of BK7-grade A glass) and two adjacent liquid chambers (3-cm path length) holding a reference liquid and a sample solution for comparative measurement. Electrodes are fabricated at the front-liquid interface so that both THG and EFISH measurements can be carried out concurrently. The coherence lengths for the harmonic generations are determined in a wedged liquid cell consisting of two crystalline quartz windows, which generates sufficient second and third harmonics for easy measurement.

With the known THG and EFISH nonlinearities and coherence lengths of the window material (BK7-grade A glass,  $\chi^{(3)}_{\text{THG}} = 4.7 \times 10^{-14}$  esu,  $l_{\text{THG}} = 16.7 \mu\text{m}$ ,  $\chi^{(3)}_{\text{EFISH}} = 3.5 \times 10^{-14}$  esu, and  $l_{\text{EFISH}} = 38.8 \mu\text{m}$ ) and the reference liquid (toluene,  $\chi^{(3)}_{\text{THG}} = 9.9 \times 10^{-14}$  esu,  $l_{\text{THG}} = 18.3 \mu\text{m}$ ,  $\chi^{(3)}_{\text{EFISH}} = 9.1 \times 10^{-14}$  esu, and  $l_{\text{EFISH}} = 73.5 \mu\text{m}$ ) as well as the measured coherence lengths of the sample solution, the solution nonlinear susceptibilities can be computed. With the measured solution properties, following the full Onsager local field model for both static and optical fields and taking the infinite dilution limit for all concentration-dependent quantities, the relevant molecular properties including the dipole moment and the hyperpolarizability are calculated.

## Results

**Synthesis and UV-Visible Spectroscopy.** The dinitrostilbenes were conveniently prepared by the reaction of 2,4-dinitrotoluene with an aldehyde in the presence of piperidine (Figure 2).<sup>12</sup> Except for one compound, the product precipitated from the reaction mixture in a pure state. It was necessary to purify the ferrocenyl compound by column chromatography. The compounds were characterized by  $^1\text{H}$  NMR and UV-visible spectroscopy and by elemental analysis. The UV-visible spectra exhibit strong charge-transfer bands, which in accord with theory shift to lower energy with increasing conjugation length and with increasing donor strength (as indicated by Hammett parameters).

### Powder Second Harmonic Generation Efficiencies.

As part of our routine screening of compounds for second harmonic generation, efficiencies of the dinitro compounds in Table IV were determined by using the Kurtz powder technique.<sup>13</sup> Most of the compounds gave negligible

**Table IV.** Summary of UV-Visible Data of 2,4-( $\text{O}_2\text{N}$ ) $_2\text{C}_6\text{H}_3\text{CH}=\text{CHX}$  and 4- $\text{O}_2\text{NC}_6\text{H}_4\text{CH}=\text{CHX}$  Compounds

X	2,4-( $\text{O}_2\text{N}$ ) $_2\text{C}_6\text{H}_3\text{CH}=\text{CHX}$			4- $\text{O}_2\text{NC}_6\text{H}_4\text{CH}=\text{CHX}$ $\lambda_{\text{max}}, \text{nm}$
	$\lambda_{\text{max}}, \text{nm}$	$\lambda_{\text{max}}, \text{nm}$	$\epsilon, \text{M}^{-1} \text{cm}^{-1}$	
2- $\text{CH}_3\text{OC}_6\text{H}_4$	381	378	17 800	368
4- $\text{CH}_3\text{OC}_6\text{H}_4$	392	384	20 800	364
2,4-( $\text{CH}_3\text{O}$ ) $_2\text{C}_6\text{H}_3$	412	404	20 600	394
$\text{C}_{16}\text{H}_9$ (1-pyrenyl)	434	436		414
4-( $\text{CH}_3$ ) $_2\text{NC}_6\text{H}_4$	475	466	23 400	424
4-( $\text{CH}_3$ ) $_2\text{NC}_6\text{H}_4$ - $\text{CH}=\text{CH}$	486	480	29 700	
$\text{C}_5\text{H}_5\text{FeC}_5\text{H}_4$	545	536	4 800	500

<sup>a</sup> In acetone. <sup>b</sup> In dioxane.

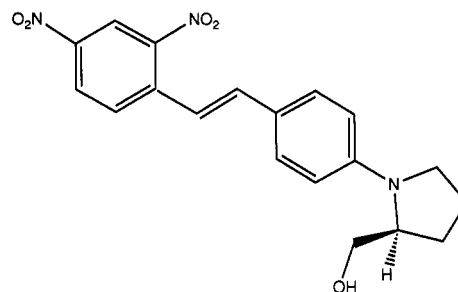


**Figure 3.** Prolinol-substituted dinitrostilbene.

powder SHG signals; however, the ferrocene compound  $\text{C}_5\text{H}_5\text{FeC}_5\text{H}_4\text{CH}=\text{CH}-2,4-\text{C}_6\text{H}_3(\text{NO}_2)_2$  gave an efficiency 21 times that of urea (1907-nm fundamental radiation). In an attempt to realize the large molecular hyperpolarizability of 4-( $\text{CH}_3$ ) $_2\text{NC}_6\text{H}_4\text{CH}=\text{CH}-2,4-\text{C}_6\text{H}_3(\text{NO}_2)_2$  (discussed below), the prolinol-substituted dinitrostilbene was synthesized (Figure 3). The chirality of the prolinol substitution guarantees noncentrosymmetric crystallization, and the pendant hydroxyl group encourages intermolecular hydrogen bonding, which has been shown to increase the probability of isolating molecules in polar space groups.<sup>14</sup> The compound exhibited a powder SHG efficiency 10 times that of urea (at 1907 nm).

**Molecular Hyperpolarizabilities.** Powder SHG efficiencies cannot generally be used to formulate molecular structure-property relationships since the macroscopic efficiency may be dominated by the orientation of the chromophores in the crystal lattice, intermolecular electronic interaction, and phase-matching properties, each of which is independent of the molecular hyperpolarizability. To understand the influence on  $\beta_u$  of the addition of a second nitro group at the 2-position to 4-nitrostilbenes, EFISH experiments were undertaken. The detailed experimental considerations have been described elsewhere,<sup>9,10</sup> although some details are given in the Experimental Section. For the purpose of this paper it is sufficient to note that the experiment relies on a partial alignment of the chromophores through interaction between the permanent molecular dipole moment and an external dc electric field, creating a quasipolar solution for second harmonic generation. The measured second harmonic intensity is related to the  $\gamma^{\text{EFISH}}$  given by

$$\gamma^{\text{EFISH}} = \gamma^e + \gamma^v + \mu\beta/5kT$$

where  $\gamma^e + \gamma^v$ , the electron and deformational contributions, are assumed to be proportional to the  $\gamma^{\text{THG}}$ , which is independently determined by THG measurements.<sup>10</sup> The constant  $\gamma^{\text{THG}}$  is determined by measurements on

(12) Prepared by analogy to trinitrostilbene: *The Chemistry of Powder and Explosives*; Davis, T. L.; Angriff Press: Hollywood, 1944; p 151.

(13) Kurtz, S. K.; Perry, T. T. *J. Appl. Phys.* **1968**, *39*, 3798.

(14) Zyss, J. S.; Nicoud, J. F.; Coquillay, M. *J. Chem. Phys.* **1984**, *4160*.

**Table V. Summary of Dipole Moments and  $\beta_\mu$  Data of 2,4-(O<sub>2</sub>N)<sub>2</sub>C<sub>6</sub>H<sub>3</sub>CH=CHX and 4-(O<sub>2</sub>N)<sub>2</sub>C<sub>6</sub>H<sub>3</sub>CH=CHX Compounds**

X	4-(O <sub>2</sub> N) <sub>2</sub> C <sub>6</sub> H <sub>3</sub> CH=CHX		2,4-(O <sub>2</sub> N) <sub>2</sub> C <sub>6</sub> H <sub>3</sub> CH=CHX	
	$\mu$	$\beta_\mu \times 10, \text{esu}$	$\mu$	$\beta_\mu \times 10, \text{esu}$
2-CH <sub>3</sub> OC <sub>6</sub> H <sub>4</sub>			5.0	12
4-CH <sub>3</sub> OC <sub>6</sub> H <sub>4</sub>	4.5	28 <sup>10</sup>	4.7	22
2,4-(CH <sub>3</sub> O) <sub>2</sub> C <sub>6</sub> H <sub>3</sub>	4.8	32 <sup>10</sup>	5.6	25
C <sub>10</sub> H <sub>8</sub> (1-pyrenyl)			8.1	11
4-(CH <sub>3</sub> ) <sub>2</sub> NC <sub>6</sub> H <sub>4</sub>	6.2	83 <sup>10</sup>	7.0	57
4-(CH <sub>3</sub> ) <sub>2</sub> NC <sub>6</sub> H <sub>4</sub> CH=CH	6.5	120 <sup>15</sup>	7.1	98
C <sub>5</sub> H <sub>5</sub> FeC <sub>5</sub> H <sub>4</sub>	3.6	34 <sup>16</sup>	4.7	20

centrosymmetric molecules with structures similar to that of the nonlinear molecule in question. From the above analysis the vector part (projected on the dipole moment) of the molecular hyperpolarizability tensor,  $\beta_\mu$ , can be determined when the molecular dipole moment,  $\mu$ , is known. EFISH measurements were performed with 1907-nm fundamental radiation ( $\lambda/2 = 953.5 \text{ nm}$ ) to minimize dispersive enhancement of  $\beta_\mu$ .

Results of EFISH and dipole moment measurements on the compounds shown in Table IV are summarized in Table V. Results for the analogous mononitro compounds are included for comparison. In general, the trends observed for the mononitro series are followed for the dinitro series. For example, the stronger donors tended to give larger  $\beta_\mu$  as did increased conjugation length. Nevertheless, the dinitro compounds did not represent an improvement (for poled polymer applications) over their mononitro analogues: for each donor substitution tried, the dipole moment of the dinitro compound was larger but the EFISH determined  $\beta_\mu$  was smaller than for its mononitro analogue.

### Discussion

**Dewar's Rules and NLO Chromophores.** It has been suggested that Dewar's rules<sup>17</sup> for predicting the spectroscopic perturbation associated with the addition of substituents to a given molecule may be useful for molecular engineering of NLO chromophores.<sup>18</sup> In particular, it was suggested that 4'-(dimethylamino)-4-nitrostilbene (DANS) was a useful starting point for engineering new nonlinear chromophores with improved transparency by judicious substitution of atoms within the  $\pi$ -system or by judicious placement of substituents.<sup>18</sup> Application of Dewar's rules to the systems described here predicts that the dinitrostilbene analogues of the nitrostilbene compounds should exhibit *higher* energy absorption bands. The opposite trend is observed; without exception the charge-transfer absorption of the dinitrostilbene appears at *lower* energy than the analogous nitrostilbene (Table IV). This is in contrast with the results previously reported for single benzene ring compounds<sup>18</sup> but is consistent with previous results on substituted azobenzenes.<sup>19</sup> It is not clear that the electronic structure of the HOMO and LUMO of the donor-acceptor stilbenes are analogous to those of a corresponding odd alternate hydrocarbons. Indeed, simple Hückel MO calculations indicate that the distribution of orbital coefficients for the HOMO and LUMO of amino-substituted stilbenes are quite different from those of the

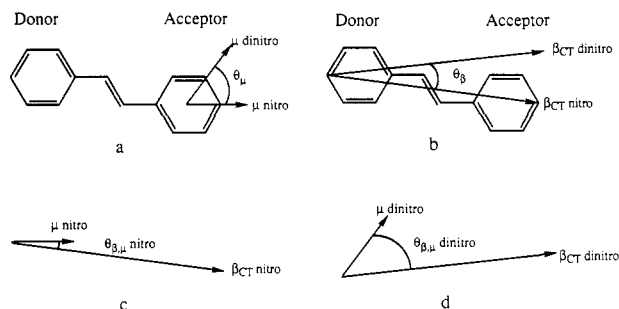


**Figure 4.** (a) Effect of multiple substitution on direction of  $\mu$ ; (b) effect of multiple substitution on direction of  $\beta_{CT}$ ; (c) angle between  $\mu$  and  $\beta_{CT}$  for nitrostilbenes; (d) angle between  $\mu$  and  $\beta_{CT}$  for dinitrostilbenes.

corresponding odd alternate hydrocarbons. Thus, one must exercise care when applying Dewar's rules to NLO chromophores.

**Molecular Hyperpolarizabilities.** At first consideration, the reduced  $\beta_\mu$  values for the dinitro compounds may be somewhat surprising, since one might reason that additional electron-withdrawing substituents on the electron-accepting part of the molecule should increase the electronic asymmetry of the molecule, leading to enhanced  $\mu$ ,  $\beta$ , and thereby  $\beta_\mu$ , particularly with both substituents in conjugation with the electron-donating group. Clearly this idea is an oversimplification and does not explain the observed results. There are two factors that may lead to the observed trends. First, a significant portion of the molecular dipole moment of nitrostilbene derivatives is due to the polarity of the nitro group itself, apart from the mesomeric contribution due to donor-acceptor interaction of the substituents. Nitrobenzene and *N,N*-dimethylaniline have dipole moments of 4.0 and 1.6 D, respectively, and 4-(CH<sub>3</sub>)<sub>2</sub>NC<sub>6</sub>H<sub>4</sub>CH=CH-4-C<sub>6</sub>H<sub>4</sub>NO<sub>2</sub> has a dipole moment of 6.2 D, only 0.6 D greater than the sum of the moments the constituent dipoles. For 4'-donor-4-nitrostilbenes, contributions from both the donor and acceptor are collinear and are parallel to the long molecular axis. For 4'-donor-2,4-dinitrostilbenes, one consequence of the 2-nitrosubstitution is to rotate the resultant dipole moment off the long molecular axis (Figure 4a). Since the EFISH determined  $\beta_\mu$  is only a vectorial projection of the hyperpolarizability tensor  $\beta$  along the dipole moment direction, its magnitude is expected to be less than the magnitude of a projection,  $\beta_{CT}$ , along the charge-transfer direction of the  $\pi$ -system when the two directions differ significantly. Thus if the charge-transfer direction and  $\beta_{CT}$  remain unchanged upon 2-nitrosubstitution, the  $\beta_\mu$  measured will be reduced by the change in dipole moment direction. If  $\beta_{CT}$  changes in both magnitude and direction but by a lesser degree than  $\mu$  (Fig. 4b),  $\beta_\mu$  will still be reduced (Fig. 4c and d). Since the dipole moment is dominated by the nitro-substitutions but  $\beta_{CT}$  is dominated by the donor-acceptor charge transfer, one would expect a larger effect on the orientation of  $\mu$  and thus a smaller  $\beta_\mu$  (as shown in Figure 4).

The second factor is the possibility of saturating the polarizability of the  $\pi$ -system with multiple strong-acceptor substitution. If the asymmetric polarizability of mononitrostilbene is close to saturation, the additional 2-nitro group could in effect compete with the 4-nitro group for oscillator strength in the excited state. Since a 2-nitro group is expected to give rise to a smaller hyperpolarizability than a 4-nitro group, this competition may diminish the overall molecular nonlinearity. The higher ground-state dipole moment and bathochromic shift of the charge-transfer band are indications that the overall charge

(15) Cheng, L. T.; Marder, S. R.; Tam, W. Manuscript in preparation.

(16) Cheng, L. T.; Tam, W.; Meredith, G. R.; Marder, S. R. *Mol. Cryst. Liq. Cryst.*, in press.

(17) Dewar, M. J. S. *J. Chem. Soc.* **1950**, 2329.

(18) Twieg, R. W. In *Nonlinear Optical Properties of Organic Molecules and Crystals*; Chemla, D. S., Zyss, J., Ed.; Academic Press: Orlando, 1987; Vol. 1, p 242.

(19) Splitter, J. S.; Calvin, M. *J. Org. Chem.* **1955**, *20*, 1086.

transfer is enhanced by the additional nitro group.

Enhancement of  $\beta$  has been realized in 2',4'-dimethoxy-4-nitrostilbene, in which the donor-group dipole moment is small. This is consistent with the effect of mutual orientation of  $\mu$  and  $\beta_\mu$ . This result and the fact that the actual nonresonant redistribution of electron density by the applied field is small suggest that the system is not at saturation polarization. Therefore, it is likely that the lower  $\beta_\mu$  results from a redirection of the dipole moment. The usable nonlinearity in electric-field aligned structures such as poled polymeric systems is represented by  $\beta_\mu$ .<sup>20</sup> Since  $\mu\cdot\beta$  for the dinitrostilbenes is comparable to those for the nitrostilbenes, the former exhibit no appreciable improvement for poled polymer applications. It is possible that some tensor components of  $\beta$  are enhanced upon multiple substitution. These enhancements may be manifested in single crystals.

**Powder SHG Efficiencies.** Even if the molecular hyperpolarizabilities of the dinitrostilbene compounds are smaller than those for the nitrostilbenes, on an absolute scale they are nonetheless large. This strongly implies that the small SHG efficiencies observed are a consequence of centrosymmetric or nearly centrosymmetric packing of the chromophores in the crystal lattice. Roughly 75% of all organic molecules crystallize in centrosymmetric space groups leading to materials with vanishing  $\chi^{(2)}$ . Since dipolar interactions provide a strong driving force for centrosymmetric crystallization, it is expected that the relatively large dipole moments of the dinitrostilbenes contribute to the unfavorable packing. Even for 4'-[2-

(hydroxymethyl)pyrrolidinyl]-2,4-dinitrostilbene, the relatively small SHG efficiency indicates that although the compound crystallizes in a noncentrosymmetric space group, the alignment of the molecules in the lattice must be far from the ideal geometry for second harmonic generation. This is in contrast to (nitrophenyl)prolinol (NPP), a yellow compound with an SHG efficiency (SH at 532 nm) about 150 times that of urea.<sup>14</sup>

**Acknowledgment.** The research described in this paper was performed by the Jet Propulsion Laboratory, California Institute of Technology, as part of its Center for Space Microelectronics Technology, which is supported by the Strategic Defense Initiative Organization, Innovative Science and Technology Office through an agreement with the National Aeronautics and Space Administration (NASA). S.R.M. thanks Professor Robert Grubbs for access to synthetic facilities at Caltech and the National Research Council and NASA for a National Research Council Resident Research Associateship at the Jet Propulsion Laboratory.

**Registry No.** (E)-2,4-(O<sub>2</sub>N)<sub>2</sub>C<sub>6</sub>H<sub>3</sub>CH=CHC<sub>6</sub>H<sub>4</sub>OMe-*o*, 129540-39-2; (E)-2,4-(O<sub>2</sub>N)<sub>2</sub>C<sub>6</sub>H<sub>3</sub>CH=CHC<sub>6</sub>H<sub>4</sub>OMe-*p*, 129540-40-5; (E)-2,4-(O<sub>2</sub>N)<sub>2</sub>C<sub>6</sub>H<sub>3</sub>CH=CHC<sub>6</sub>H<sub>4</sub>NMe<sub>2</sub>-*p*, 61599-67-5; (E,E)-2,4-(O<sub>2</sub>N)<sub>2</sub>C<sub>6</sub>H<sub>3</sub>CH=CHCH=CHC<sub>6</sub>H<sub>4</sub>NMe<sub>2</sub>-*p*, 129540-43-8; (E)-2,4-(O<sub>2</sub>N)<sub>2</sub>C<sub>6</sub>H<sub>3</sub>CH=CH(C<sub>6</sub>H<sub>4</sub>FeC<sub>5</sub>H<sub>5</sub>), 129540-46-1; *o*-MeOC<sub>6</sub>H<sub>4</sub>CHO, 135-02-4; *p*-MeOC<sub>6</sub>H<sub>4</sub>CHO, 123-11-5; 2,4-(CH<sub>3</sub>O)<sub>2</sub>C<sub>6</sub>H<sub>3</sub>CHO, 613-45-6; 4-(CH<sub>3</sub>)<sub>2</sub>NC<sub>6</sub>H<sub>4</sub>CHO, 100-10-7; (E)-4-(CH<sub>3</sub>)<sub>2</sub>NC<sub>6</sub>H<sub>4</sub>CH=CHCHO, 20432-35-3; C<sub>5</sub>H<sub>5</sub>FeC<sub>5</sub>H<sub>4</sub>CHO, 12093-10-6; (E)-1,2-bis(2,4-dimethoxyphenyl)ethylene, 129540-41-6; (E)-1-(2,4-dinitrophenyl)-2-(1-pyrenyl)ethylene, 129540-42-7; 4'-[2-(hydroxymethyl)pyrrolidinyl]-2,4-dinitrostilbene, 129540-44-9; 1-pyrenecarboxaldehyde, 3029-19-4; 4'-[2-(hydroxymethyl)pyrrolidinyl]benzaldehyde, 129540-45-0; 2,4-dinitrotoluene, 121-14-2.

(20) Singer, K. D.; Sohn, J. E. *Lalama, S. J. Appl. Phys. Lett.* 1986, 49, 248.

## Solid-Phase Equilibria for Metal-Silicon-Oxygen Ternary Systems. 1. Mg, Ca, Sr, and Ba

Haojie Yuan and R. Stanley Williams\*

Department of Chemistry and Biochemistry and Solid State Science Center, University of California, Los Angeles, Los Angeles, California 90024-1569

Received December 20, 1989

Ternary-phase diagrams for systems of the type M-Si-O, where M = Mg, Ca, Sr, and Ba, have been derived. These phase diagrams can be used to understand experimental results reported in the literature for thin-film chemical reactions of SrO on Si and provide guides in designing stable structures that involve different materials in intimate contact. These particular phase diagrams are especially relevant for investigating the chemical stability of interfaces between SiO<sub>2</sub> and the oxide superconductors.

### Introduction

Chemical reactions that occur at the interfaces separating different solids are scientifically interesting and technologically important. Many studies have shown that one of the first steps in understanding and controlling interfacial chemistry is to map the bulk-phase diagram containing the elements of interest.<sup>1-6</sup> These phase diagrams can be used to predict the occurrence of reaction products or, conversely, the stability of the phases present at the interfaces between different materials. Hence,

bulk-phase diagrams can provide guides in designing thin-film structures and in selecting candidate materials to form chemically stable interfaces.

In this work, we derived phase diagrams for systems of the type M-Si-O, where M = Mg, Ca, Sr, and Ba. These

(1) Schwartz, G. P.; Gaultieri, G. J.; Griffiths, J. E.; Thurmond, C. D.; Schwartz, B. *J. Electrochem. Soc.* 1980, 127, 2488.

(2) Thurmond, C. D.; Schwartz, G. P.; Kammlott, G. W.; Schwartz, B. *J. Electrochem. Soc.* 1980, 127, 1366.

(3) Schwartz, G. P. *Thin Solid Films* 1983, 103, 3.

(4) Beyers, R. *Mater. Res. Soc. Proc.* 1985, 47, 143.

(5) Tsai, C. T.; Williams, R. S. *J. Mater. Res.* 1986, 1(2), 352.

(6) Pugh, J. H.; Williams, R. S. *J. Mater. Res.* 1986, 1(2), 343.

\* To whom correspondence should be addressed at the Department of Chemistry and Biochemistry.